

# LARNITE POWDERS AND LARNITE/SILICA AEROGEL COMPOSITES AS EFFECTIVE AGENTS FOR CO<sub>2</sub> SEQUESTRATION BY CARBONATION

*A. Santos,<sup>(1)</sup> M. Ajbary,<sup>(2)</sup> V. Morales-Flórez,<sup>(2)</sup> A. Kherbeche,<sup>(3)</sup> M. Piñero,<sup>(4)</sup> L.  
Esquivias<sup>(5)</sup>*

<sup>(1)</sup> Departamento de Ciencias de la Tierra, Universidad de Cádiz, Spain.

<sup>(2)</sup> Departamento de Física de la Materia Condensada, Universidad de Cádiz, Spain.

<sup>(3)</sup> Université Sidi Mohamed Ben Abdellah, École Supérieure de Technologie, Maroc.

<sup>(4)</sup> Departamento de Física Aplicada, Universidad de Cádiz, Spain.

<sup>(5)</sup> Departamento de Física de la Materia Condensada. Universidad de Sevilla. Spain.

## **Abstract**

This paper presents the results of the carbonation reaction of two sample types: larnite (Ca<sub>2</sub>SiO<sub>4</sub>) powders and larnite/silica aerogel composites. In both samples the larnite acts as an active phase in a process of ex-situ mineral sequestration. First, larnite powders were synthesized by the reaction of colloidal silica and calcium nitrate in the presence

of ethylene glycol. Then, to synthesize the composites, the surface of the larnite powders was chemically modified with 3-aminopropyltriethoxysilane (APTES), and later this mixture was added to a silica sol previously prepared by hydrolysis and polycondensation of tetraethoxysilane (TEOS). The resulting humid gel was dried in an autoclave under supercritical conditions for the ethanol. The texture and chemical composition of the powders and composites (containing 67% -34 wt% of CaO respectively) were characterized.

The carbonation reaction of both types of samples was evaluated by means of X-ray diffraction and thermogravimetric analysis. Both techniques confirm the high efficiency of the reaction at room temperature and atmospheric pressure. A complete transformation of the silicate into carbonate resulted after submitting the samples to a flow of pure CO<sub>2</sub> for 15 min. This indicates that for this reaction time, 1 Tm of larnite could eliminate between 620 and 670 kg of CO<sub>2</sub>. The grain size, porosity, and specific surface area are the factors controlling the reaction.

Keywords: Larnite, Larnite-silica aerogel composites, CO<sub>2</sub>, Carbonation, mineral sequestration

## 1. Introduction

### 1.1. General considerations

An important strategy in carbon capture and storage (CCS) is long-term geological storage. Such a technology consists of capturing gaseous CO<sub>2</sub> from emissions sources and storing CO<sub>2</sub> in depleted oil and gas fields or equivalent geological trap situations, with the side effect of enhancing oil production. However, this method bears the risk of possible diffusion of the CO<sub>2</sub> via rock cracks and other zones of weakness allowing portions of the injected CO<sub>2</sub> to re-enter the atmosphere. This problem can be solved if the injected CO<sub>2</sub> is transformed by carbonation into a stable insoluble inorganic mineralogical phase [1,2]. This reaction is the safest method of CO<sub>2</sub> storage. Consequently, it is suitable for use when the priority is the management of the environmental risks, because it ensures that the CO<sub>2</sub> captured and stored remains isolated from the atmosphere and biosphere.

In the carbonation reaction, the CO<sub>2</sub> reacts with alkaline-earth silicates, forming the corresponding carbonate and silica as by-products. However, these are low rate reactions that need to be accelerated for a useful process of massive carbonation for CO<sub>2</sub> sequestration. Among the researches carried out to overcome this drawback can be found studies on carbonation in aqueous media and the influence of several factors such as the mineral grain reactive surface [3, 4, 5], the use of acidic media for the extraction of the divalent cation [6], and the carbonation reaction under CO<sub>2</sub> supercritical conditions [7, 8]. All things considered, in aqueous systems the divalent cation dissolution from the precursor silicates seems to be the main rate-limiting step, and most research efforts have been devoted to finding ways to speed up the cation extraction from the precursor materials [9].

## 1.2. Specific considerations

Other important aspects of carbonation to consider are the type of silicate and the amount that represents the divalent cation relative to the silicate composition. The inhibiting effect induced by the formation of a passivating layer on the reacted mineral surface is also relevant to carbonation efficiency [10]. These facts are the subject of this paper because the higher the cation content, the higher the sequestration capacity of the material. Secondly, avoiding the passivating layer will result in shortening the reaction time and lowering the cost of the sequestration process.

It is known that among the silicates, those of calcium present the highest carbonation reaction rate [7]. Wollastonite, which contains 42–44 wt % of CaO, has been widely used in early research; however the performance of larnite, which contains 64–67 wt % of CaO, (~50% more than wollastonite) has been insufficiently studied, probably due to its scarcity. Three polymorphic forms of dicalcium silicate have been recognized in geologic outcrops [11]. The larnite mineral,  $\beta$ -Ca<sub>2</sub>SiO<sub>4</sub>, also known as belite, is a major constituent of Portland cement [12].

We present here the synthesis of two types of sample: larnite powders and larnite/silica aerogel composites. The methods used for their synthesis are known [13,14,15]; they allow homogeneous materials to be obtained at a temperature lower than the standard methods applied to the fabrication of the individual components of the cement.

In this work, as described in previous studies [15], we take advantage of a general feature of silica aerogels: their high specific surface area as an efficient agent to fixate CO<sub>2</sub> when a divalent cation silicate is installed as an active phase in the silica aerogel matrix. On the other hand, the silicate synthetic samples, including products of solid waste incineration [16,17] could be a sustainable alternative to the natural silicates. This

is because they avoid the impact of mineral extraction on a massive scale, pre-treatment of samples, and transport to the CO<sub>2</sub> source and, in general, the synthetic samples are more reactive than the natural ones [18]. In this sense, these methods of synthesis allow the control of important parameters such as particle size at the scale of nanometers, porosity, and specific surface area. These parameters play an important role in increasing the reaction rate, even at room temperature and atmospheric pressure [15,19]. Larnite carbonation presents a particular additional advantage: this carbonation can vary the properties of the materials, reducing their environmental impact and increasing their value. For example, recycling CO<sub>2</sub> in cement can reduce the curing time and improve the strength of the material [20,21].

This paper is a part of a larger study: in the first stage, the aims are to speed up the carbonation reaction rate and increase the CO<sub>2</sub> fixation capacity. In this regard, the textural characteristics of the samples can help to overcome the inhibiting effects of the passivating layer created on the mineral surface. The second stage is the optimization of the synthesis conditions to reduce the cost, which is undoubtedly the more important drawback with respect to alternatives based on natural products. In this sense, since the aerogels are obtained by elimination of the solvent under supercritical conditions, an important issue would be to eliminate stages in the processing of composites. This would be possible, if the carbonation reaction takes place at the same time that the supercritical drying when the solvent is the CO<sub>2</sub>.

## **2. Processing and experimental methods**

### **2.1 Synthesis of larnite powders**

Larnite powders were obtained from a mixture of colloidal silica and calcium nitrate tetrahydrate. This mixture was realized in aqueous solution in the presence of ethylene

glycol under vigorous magnetic stirring. The gel obtained by means of evaporation is allowed to dry and heat-treated.

Thus, a 0.46 M solution of Ludox® AM-30 (6 g in 56 mL of distilled water) was added to a 1 M  $\text{Ca}(\text{NO}_3)_2 \cdot 4\text{H}_2\text{O}$  (Aldrich Chemical Co, USA; purity 99%) aqueous solution (14.152 g in 60 mL of distilled water). After 10 min stirring, 104 mL of diluted (5%) ethylene glycol (Panreac Química, SA) were added. The mixture was heated to 100 °C with magnetic stirring until the solvent evaporated completely. The Ca/Si molar ratio of the resulting gel was 2. This sample was called “larnite 2”.

This product was placed in an oven at 100 °C for 48 h more, then ground, and finally the resulting powders were heat-treated in a furnace at 600 °C for 1 h (300 °C/h heating rate).

A second type of gel was prepared in a similar way, but varying the amounts of nitrate and ethylene glycol. In this case, 7.07 g of calcium nitrate tetrahydrate were dissolved in 60 mL of distilled water and only 67 mL of the aqueous solution (5%) of ethylene glycol were added to the Ludox-nitrate mixture. The Si/Ca molar ratio of the resulting gel was 1, and the gel was therefore called “larnite 1”. The rest of the processing was the same as before.

## **2.2 Processing of the larnite/silica aerogel composites.**

The larnite powders' surfaces were chemically modified with 3-aminopropyltriethoxysilane (APTES, Fluka, France;  $\geq 97\%$ ) to facilitate and stabilize a colloidal dispersion into the precursor sol of the host matrix. The APTES/powder was dispersed in ethanol, and the mixture was submitted to ultrasound action for a few minutes and then allowed to dry. Then, this mixture was dispersed in a sol of tetraethoxysilane (TEOS, Merck, Germany; purity  $\geq 99\%$ ). This stage allows control of

the gelling time, which must be short enough to avoid the decantation of the powders.

Once gelled and aged in ethanol, the humid gel was placed in an autoclave.

To synthesize the composites 1, first a sol was prepared by hydrolysis and polycondensation of tetraethoxysilane (1.66 mL 0.5N nitric acid to 5 mL TEOS, in 2 mL of ethanol), ultrasonically assisted with  $670 \text{ J/cm}^3$  of ultrasound energy from a sonifier (KONTES) operating at 20 kHz with a power output of 16 W. The resulting sol was distributed in three containers to which 2.5, 5, and 10 g of the APTES/larnite 1 mixture were added, respectively. The mixtures were also submitted to ultrasound for a few minutes. After this, the resulting humid gels were placed in an autoclave to obtain the aerogels by supercritical extraction of the solvent (255 °C and 90 bar), which was mostly ethanol. Finally, the composite materials were heat-treated in a furnace at 600 °C for 1 h (300 °C/h heating rate). The CaO contents of these three larnite/silica aerogel composites were determined (composites 1A, 1B, and 1C).

Only one type of composite 2 was prepared with the larnite 2 sample. This composite was obtained by the addition of 15 g of the APTES/larnite 2 mixture to a sol of TEOS previously prepared as described above. The rest of the processing was similar to that of the composite 1 series.

### **2.3 Samples characterization**

Prior to examining their capacity for CO<sub>2</sub> sequestration, the samples were characterized. The compositional and textural features of the samples were determined by X-ray fluorescence (Bruker S4 Pioneer model) and isothermal nitrogen adsorption in an automatic device (Sorptomatic 1990, CE Instruments), and the Brunauer–Emmett–Teller (BET) method was applied to calculate their specific surface areas. X-ray diffraction (XRD) experiments were performed using a Bruker diffractometer (D8 Advance) with graphite monochromator and Cu K<sub>α</sub> radiation. The intensities were

measured in a  $2\theta$  range ( $5^\circ$ – $50^\circ$ ) with a step of  $0.2^\circ$  and a counting time of 5 s per step. EVA and FULLPROF software were employed for the analysis of the crystallization products (larnite powders and carbonates). In addition, the quantity of resulting carbonate was determined by thermogravimetric analysis (TGA) in air (Setaram Setsys 16/18), heating from  $20^\circ\text{C}$  to  $900^\circ\text{C}$  at  $10^\circ\text{C}/\text{min}$  and their time derivative (DTG) were calculated. Finally, the samples were examined using scanning electron microscopy (SEM) and transmission electron microscopy (TEM). The observations were performed by using, respectively, the Field Emission Synton Scanning Electron Microscope with a resolution of 1.5 nm installed in the Central Science and Technology of the University of Cadiz and the H800 from Hitachi installed in the Research, Technology and Innovation Centre of the University of Seville (CITIUS).

#### **2.4 Carbonation process and by-product analysis**

To compare the carbonation efficiency between powder and composites samples, the carbonation procedure was only conducted using two types of samples: the larnite 2 and the composite 1C samples, containing 67 and 40 wt % of CaO, respectively. The processes followed for both samples were similar:

0.5 g of sample were ground and then dispersed in 25 mL of distilled water in a glass reactor using magnetic stirring. The pH of the water after dispersing the samples was higher than 10.5. The reactor has two valves, for the inlet and outlet of gas. The dispersion was subjected to a steady pure  $\text{CO}_2$  bubbling for 15 min at room temperature and atmospheric pressure, whilst continuing to stir. During this time, the pH decreased to between 6.5 and 7. Finally, the reaction by-product was analyzed by XRD and TGA to examine the larnite to calcium carbonate conversion efficiency. Part of the by-product was dried, mixed, and then heat-treated in a furnace at  $900^\circ\text{C}$  for 1 h ( $300^\circ\text{C}/\text{h}$  heating rate). The sample was analyzed by XRD again.



### 3. Results and discussion

The chemical compositions and the specific surface areas of both samples types are shown in Table 1. In the analysis BET of the composites, the reference values of the specific surface area correspond to the silica aerogel ( $\sim 1\,000\text{ m}^2/\text{g}$  [15]). With respect to this value, the specific surface area decreases as the concentration of the active phase increases.

In both samples, the characteristic porous structure and nanometric size are observed (Figure 1). In the case of the powders, the samples treated at  $600\text{ }^\circ\text{C}$ , not only dendritic morphologies, but also particulate aggregates are observed due to the beginning of the sintering. The composite shows a characteristic morphology of particles coating by the aerogel matrix.

A TEM micrograph of the larnite 2 composite is shown in Figure 2. The mixing of the co-existing silica matrix and larnite particles can be appreciated. The larnite particles of a few tenths of a nanometer in size are coated by fine aerogel phase. Accordingly, the synthetic issue makes it possible to obtain textural features (particle size and specific surface area) appropriate for the carbonation process that are impossible to find in natural compounds.

The mineralogical characterization is carried out from the XRD pattern shown in Figure 3. The phase evolution sequence with the temperature of the larnite 2 samples heat-treated at  $600$  and  $1\,000\text{ }^\circ\text{C}$  can be seen. At  $600\text{ }^\circ\text{C}$  the peaks are broad, corresponding to the early stage of crystal nucleation and growth. The pattern permits identification of the major presence of the  $\alpha$  and  $\beta$  phases of the dicalcium silicate (Powder Diffraction File, PDF: 020-0237 and 083-0461, respectively). Besides a certain amount of an amorphous phase, the existence of a small amount of tobermorite (hydrated calcium silicate, PDF: 089-6458) can be seen. In the pattern from the sample

heat-treated at 1 000 °C it can be observed that both the amorphous phase and hydrated silicate disappear. At this temperature, the amount of  $\alpha$ -Ca<sub>2</sub>SiO<sub>4</sub> decreases and the main component of the dicalcium silicate is  $\beta$ -Ca<sub>2</sub>SiO<sub>4</sub>. As a consequence of the calcium silicate transformation, wollastonite 1T (PDF: 084-0651) appears at this temperature as well.

The aim of this monitoring is the unambiguous identification of the powders heat-treated at 600 °C because it is these powders that have been carbonated, whether directly or encapsulated in an aerogel matrix. Both phases ( $\alpha$  and  $\beta$ ) of the dicalcium silicate are present, making identification difficult since their more important reflections overlap.

The mineralogical composition of the composites is the same as that recognized in the powders heat-treated at 600 °C. However, in these composites the mineralogical phases do not appear as sharply as in the powders because there is an amorphous background produced by the silica aerogel matrix (Figure 4) that makes the phase identification difficult. Nevertheless, the main reflections can be identified and they feature the same phase as the powders.

The synthesized powders were further tested for CO<sub>2</sub> fixation both alone and hosted in an aerogel matrix. Figure 5 shows, respectively, the XRD patterns of the larnite 2 and composite 1C samples after 15 min of carbonation reaction inside the reactor. Contrary to the protocol followed in our former work on wollastonite carbonation [15, 19, 22], the samples were analyzed immediately after the end of the experiment instead of leaving them to stand in the reactor for several hours. In both cases it was possible to identify the calcium carbonate (CaCO<sub>3</sub>) polymorphs calcite and vaterite (PDF: 086-0174 and 074-1867, respectively), which belong to the same structural family. The

vaterite is also known as mu-calcium carbonate ( $\mu\text{-CaCO}_3$ ). Unlike the calcite, vaterite is thought to be metastable. It is worth noting the absence of any trace of calcium silicates such as larnite and tobermorite.

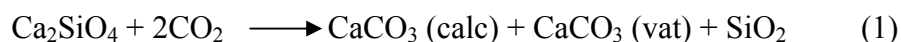
The carbonation by-products were observed with SEM (Figure 6). In the micrograph shown in Figure 6a, characteristic rhombohedral calcite crystals (1–3  $\mu\text{m}$  in size) can be observed. They appear mostly isolated and separate, but in some cases intergrowth of calcite/silica (silica as a carbonation by-product counterpart) can be also observed. The silica is recognized because the EDS analysis indicates the presence of Si.

In Figure 6b the other carbonated component (vaterite) can be observed. This figure shows particles with a typical spherulitic morphology, which is composed of framboidal aggregate broken into parts [23]. The nanometric crystallites that compose the inner part of the broken framboidal structure can be made out.

When the sample is left to stand for 12 h in the reactor, the metastable carbonate (vaterite) transforms into stable carbonate (calcite). This transformation can be observed in Figure 7, which shows the XRD patterns of the carbonation by-products analyzed immediately after stopping the gas bubbling and by-products left in the rest in the reactor.

As can be inferred from the diffraction pattern of the by-products immediately after the end of the carbonation experiment (Figure 5), the silicate to carbonate transformation rate was 100%. Figure 8 shows the weight loss of the larnite 2 (a) and composite 1C (b) carbonation by-products when they are heated from room temperature to 900 °C at 10 °C/min. The transformation rate calculated from the x-ray pattern is supported by the evaluation of the reaction conversion efficiency from the weight losses observed in the TGA experiments. According to a previous analysis, a pure carbonate decomposes between ~400 °C and ~750 °C in two bursts, as observed in the differential

curves (DTG). The first burst, found between 400 °C and 600 °C, is related to the vaterite decomposition, whereas the second, between 535 °C and 750 °C, corresponds to the calcite decomposition. In the carbonation reaction, one mol of larnite is converted into one mol of calcite and one mol of vaterite according to:



According to the CaO contents of the larnite 2 (67 wt % of CaO) and the composite 1C (43–44 wt % of CaO) samples, the maximum theoretical weight losses caused by release of the reacted CO<sub>2</sub> would be 34% and 24–25%, respectively. The actual weight losses are consistent with these percentages. Therefore, the efficiency of the carbonation reaction, that is, the amount of carbonate formed after submitting the samples to 15 min of gas flow, is estimated to be 100%.

Having obtained the by-products (carbonate and silica) of each sample, they were heat-treated separately as described in the experimental section. The resulting product was analyzed by XRD and identified as mainly larnite with minor amounts of wollastonite. The relative amounts of the two minerals depend on the carbonate/silica ratio of the by-products. This process and its result are not exclusive to the compounds that were the object of this study but can be extended to any other compounds that can be carbonated with the same carbonation by-products.

In summary, the samples studied have a high capacity for CO<sub>2</sub> fixation and the carbonation reaction is highly efficient during a short reaction time. It is worth emphasizing that the experiments were carried out at room temperature and under atmospheric pressure. The reasons for such high performance results must be found in the optimization of structural parameters that directly influence the mineral carbonation: the nanometric size of the active phase particles and the high specific surface area of the samples that favor the rapid dissolution of the silicate and, accordingly, the liberation of

calcium cations. This explanation, already given in our previous studies of wollastonite [15], could justify the sharp pH rise at the moment the samples make contact with water. Finally, these structural characteristics, together with the high porosity, could help the silicate particles to be consumed rapidly during the reaction. This avoids the formation of the inhibiting passivating layer on the silicate mineral surface.

At the same time, although intergrowth of silica/carbonate exists, the fast liberation of the Ca to the bulk solution explains a precipitation from the bulk, causing the appearance of a large amount of gappy crystals of different morphologies. Furthermore, fast calcium liberation could permit high supersaturation in the reactor and, accordingly, a reaction rate high enough to justify the formation of a metastable phase such as vaterite.

Finally, the cycle is completed with the heat-treatment of the by-products. That is, an aerogel/larnite powder composite is elaborated starting from a raw material (larnite). When these materials, whether larnite powders or composites, are subjected to a CO<sub>2</sub> flow, they carbonate fully after 15 min. Heat-treating the resulting by-products yields a final product, the majority of which is the starting product.

#### **4. Conclusions**

1. Two types of samples have been synthesized from gels: larnite powders and silica aerogel/larnite powder composites.
2. The processing makes it possible to obtain larnite powders of fine grain size and high specific surface areas and porosity of the composites. These structural features result in a high reactivity product because they avoid the formation of a reaction-inhibiting layer on the mineral surface.

3. The processing has permitted the synthesis of dicalcium silicate (larnite) that has a CO<sub>2</sub> fixation capacity 50% higher than that of wollastonite.
4. The reaction turns out to be highly efficient (100%) in only 15 min of gas flow at room temperature and under atmospheric pressure.
5. These characteristics make these samples very efficient agents for CO<sub>2</sub> fixation and elimination.

### **Acknowledgements**

We are grateful for the support of the Spanish Ministerio de Medio Ambiente and the Ministerio de Educación y Ciencia through the project A266/2007/3-11.1, which is already completed, and Project MAT2005-01583, respectively. They permitted us to buy part of the infrastructure used in this work and enabled us to partially support the living expenses of Mohamed Ajbary. We also thank the Consejería de Innovación Ciencia y Empresa of the Junta de Andalucía (Spain) for the annual grant (TEP115).

Table 1

Sample	Chemical composition		Textural characteristics
	CaO %	SiO <sub>2</sub> %	Specific surface area (m <sup>2</sup> /g)
Larnite 2	65–67	34–32	39
Larnite 1	50–55	50–45	–
Composite 1C	43–44	54.98	53
Composite 1B	40.48	58.38	115
Composite 1A	34.33	64.7	258
Composite 2	61–62	39–38	40

## Figure Captions

Figure 1. SEM micrograph of larnite 2 (a) and composite 1C (b) samples. Both heat-treated at 600°C.

Figure 2. TEM micrograph of composite 1C.

Figure 3. XRD patterns of the larnite 2 sample treated at 600 °C and 1000 °C. Identification of the components.

Figure 4. Comparison of the XRD pattern between samples of larnite 2 (grey line) and composite 1C (black line). Both heat-treated at 600°C.

Figure 5. XRD patterns of the larnite 2 powders and composite 1C after 15 min of reaction in the reactor. Identification of the by-products

Figure 6. SEM micrograph of the by-product after samples carbonation. (a) calcite crystals and silica (b) vaterite crystals.

Figure 7. XRD pattern of the by-products immediately after the end of the carbonation experiment (grey line) and left to rest in the reactor for 12 h (black line).

Figure 8. TGA and DTG curves of the carbonation by-products of the larnite 2 (a) and composite 1C (b). Heating rate: 10 °C/min



## References

---

- [1] W. Seifritz, "CO<sub>2</sub> Disposal by Means of Silicates". *Nature* **345** (1990) 486.
- [2] K.S. Lackner, "A Guide to CO<sub>2</sub> Sequestration". *Science* **300** (2003) 1677.
- [3] R. Zevenhoven, S. Eloneva, S. Teir, "Chemical Fixation of CO<sub>2</sub> in Carbonates: Route to Valuable Products and Long-term Storage" *Catal. Today* **115** (2006) 73–79.
- [4] T. Kojima, A. Nagamine, N. Ueno, S. Uemiya, "Absorption and Fixation of Carbon Dioxide by Rock Weathering". *Energy Convers. Management* **38** (1997) 461–466.
- [5] J.C.-S.Wu, J.-D.Sheen, S.-Y.Chen, Y.-Ch. Fan, "Feasibility of CO<sub>2</sub> Fixation Via Artificial Rock Weathering", *Ind. Eng. Chem. Res.* **40** (2001) 3902–3905.
- [6] M. Kakizawa, A. Yamasaki, Y. Yanagisawa, "A New CO<sub>2</sub> Disposal Process Via Artificial Weathering of Calcium Silicate Accelerated by Acetic Acid", *Energy* **26** (2001) 341–354.
- [7] C.Y. Tai, W.-R. Chen, S.-M. Shih, "Factors Affecting Wollastonite Carbonation under CO<sub>2</sub> Supercritical Conditions", *AIChE Journal* **52** (2006) 292–299.
- [8] W.K. O'Connor, D.C. Dahlin, G.E. Rush, C.L. Dahlin, W.K. Collins, "Carbon Dioxide Sequestration by Direct Mineral Carbonation: Process Mineralogy of Feed and Products", *Minerals & Metallurgical Processing* **19** (2002) 95–101.
- [9] W.J.J. Huijgen, R.N.J. Comans, "Mechanisms of Aqueous Wollastonite Carbonation as a Possible CO<sub>2</sub> Sequestration Process". *Chemical Engineering Science* **61** (2006) 4242–4251.

- 
- [10] H. Bearat, M.J. Mckelvy, A.V.G. Chizmeshya, D. Gormley, R. Nuñez, R.W. Carpenter, K. Squires, G.H. Wolf, “Carbon Sequestration Via Aqueous Olivine Mineral Carbonation: Role of Passivating Layer Formation”, *Environmental Science & Technology* **40** (2006) 4802–4806.
- [11] T. E. Bridge, “Bredigite, larnite and  $\gamma$  dicalcium silicates from marble canyon”, *American Mineralogist* **51**(1966) 1766-1774.
- [12] U.S Department of Transportation. Federal Highway Administration.  
<http://www.fhwa.dot.gov/infrastructure/materialsgrp/cement.html>. Last accessed November 12<sup>th</sup> 2008.
- [13] S.H. Hong, J.F. Young, “Hydration Kinetics and Phase Stability of Dicalcium Silicate Synthesized by the Pechini Process”, *J. Am. Ceram. Soc.* **82** (1999) 1681–1686.
- [14] R. Chrysafi, T. Perraki, G. Kakali, “Sol-Gel Preparation of  $2\text{CaO}\cdot\text{SiO}_2$ ”, *J. Eur. Ceram. Soc.* **27** (2007) 1707–1710.
- [15] A. Santos, J.A. Toledo-Fernández, R. Mendoza-Serna, L. Gago-Duport, N. Rosa-Fox, M. Piñero, L. Esquivias, “Chemically Active Aerogel-Wollastonite Composites for  $\text{CO}_2$  Fixation by Carbonation Reactions”, *Ind. Eng. Chem. Research* **46** (2007) 103–107. DOI: 10.1021/ie0609214.
- [16] E. Rendek, G. Ducom, P. Germain, “Carbon Dioxide Sequestration in Municipal Solid Waste Incinerator (MSWI) Bottom Ash”, *J. Hazard. Mater.* **128** (2006) 73–79.
- [17] G. Montes-Hernández, R. Pérez-López, F. Renard, J.M. Nieto, L. Charlet, “Mineral Sequestration of  $\text{CO}_2$  by Aqueous Carbonation of Coal Combustion Fly-Ash”, *J. Hazard. Mater.* (2008). DOI: 10.1016/J.Jhazmat.200804.104.

- 
- [18] O. Shtepenko, C. Hills, A. Brough, M. Thomas, “The Effect of Carbon Dioxide on  $\beta$ -dicalcium Silicate and Portland Cement”, *Chemical Engineering Journal* **118** (2006) 107–118.
- [19] A. Santos, M. Ajbary, J.A. Toledo-Fernández, V. Morales-Flórez, A. Kherbeche, L. Esquivias, “Reactivity of CO<sub>2</sub> Traps in Aerogel-Wollastonite Composites”, *J. Sol-Gel Sci. Technol.* **48** (2008) 224–230. DOI: 10.1007/s10971-008-1719-y.
- [20] J.M. Bukowski, R.L. Berger, “Reactivity and Strength Development of CO<sub>2</sub> Activated Non-hydraulic Calcium Silicates”, *Cem. Conc. Res.* **9** (1979) 57–68.
- [21] M. Fernández Bertos, S.J.R. Simons, C.D. Hills, P.J. Carey, “A Review of Accelerated Carbonation Technology in the Treatment of Cement-Based Materials and Sequestration of CO<sub>2</sub>”, *J. Hazard. Mater.* **112** (2004) 193–205.
- [22] A. Santos, M. Ajbary, A. Kherbeche, M. Piñero, N. de la Rosa-Fox, L. Esquivias, “Fast CO<sub>2</sub> Sequestration Aerogel Composites”, *J. Sol-Gel Sci. & Technol.* **45** (2008) 291–297. DOI: 10.1007/s10971-007-1672-1.
- [23] G. Nehrke, P. Van Capellen, “Framboidal Vaterite Aggregates and Their Transformation into Calcite: A Morphological Study”, *J. Crystal Growth* **287** (2006) 528–530.

6. Figure(s)

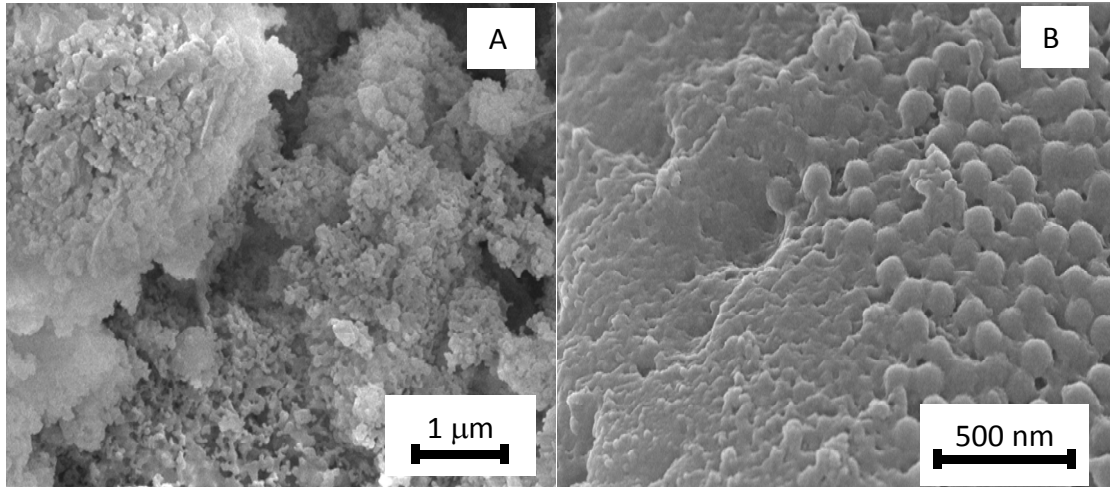


Figure 1

6. Figure(s)

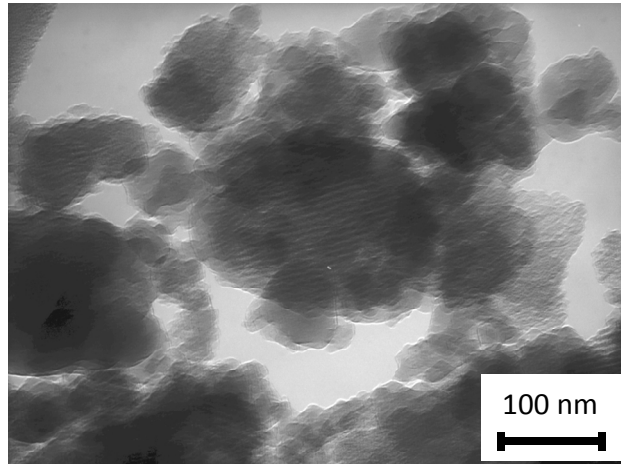
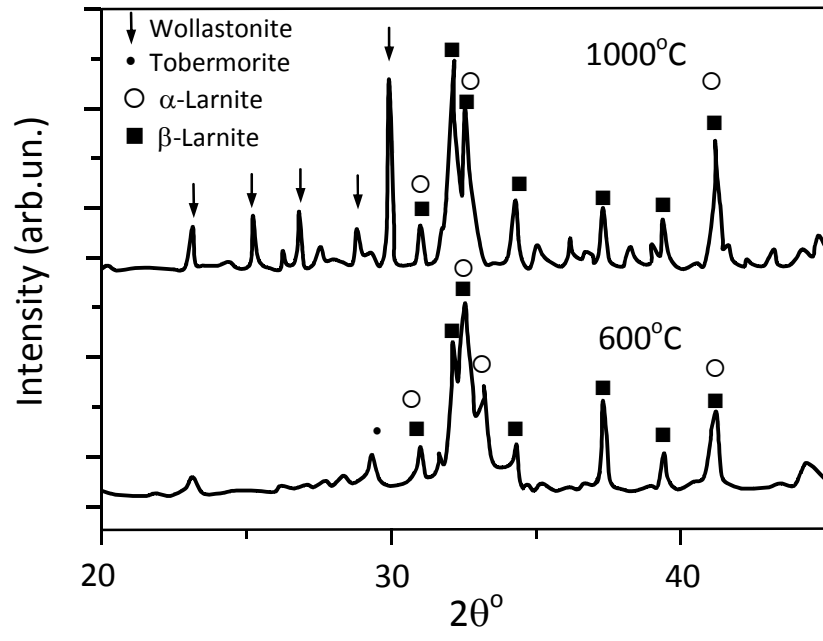


Figure 2

6. Figure(s)



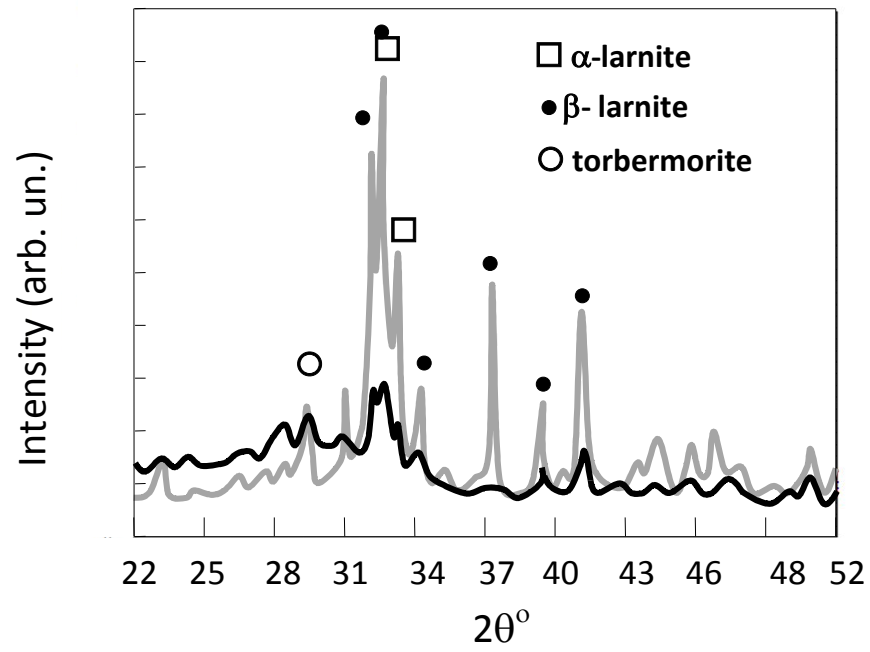


Figure 4

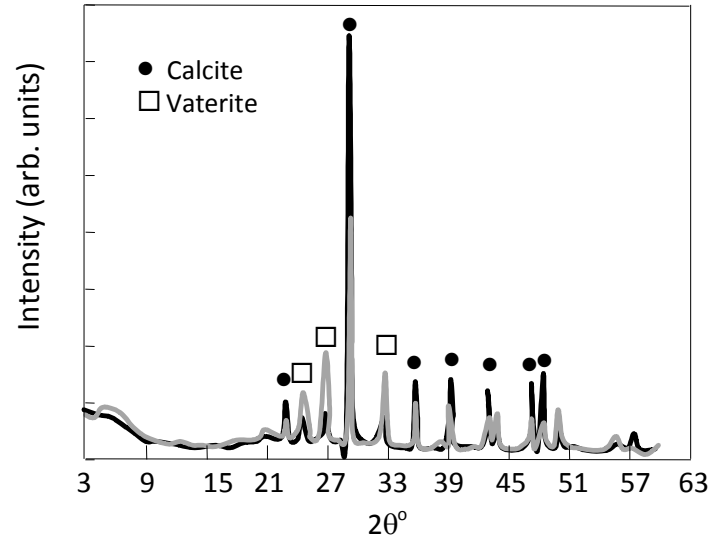


Figure 5



6. Figure(s)

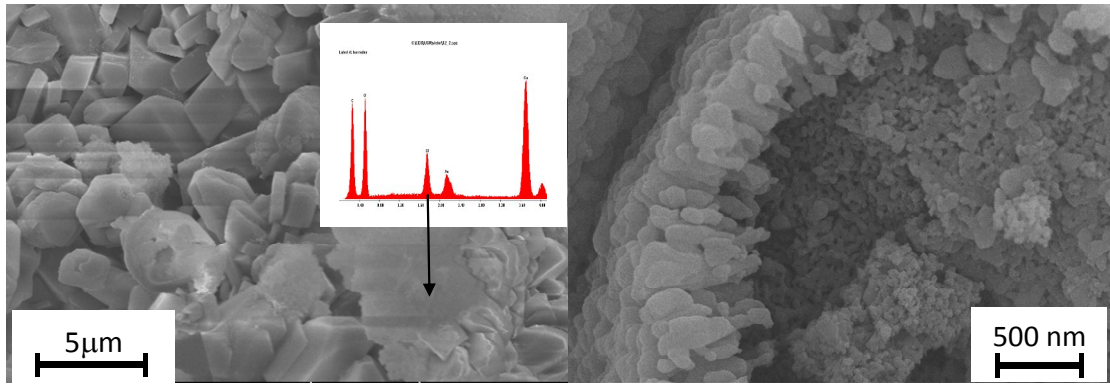


Figure 6 a and b

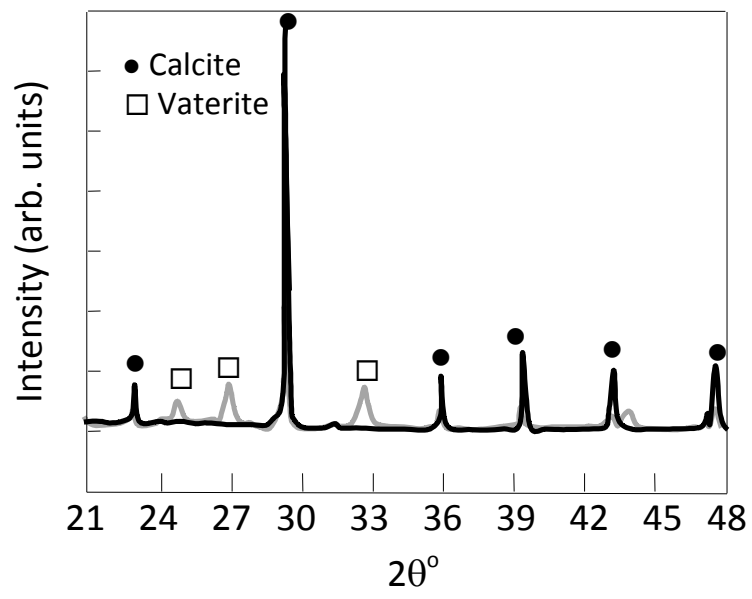


Figure 7

6. Figure(s)

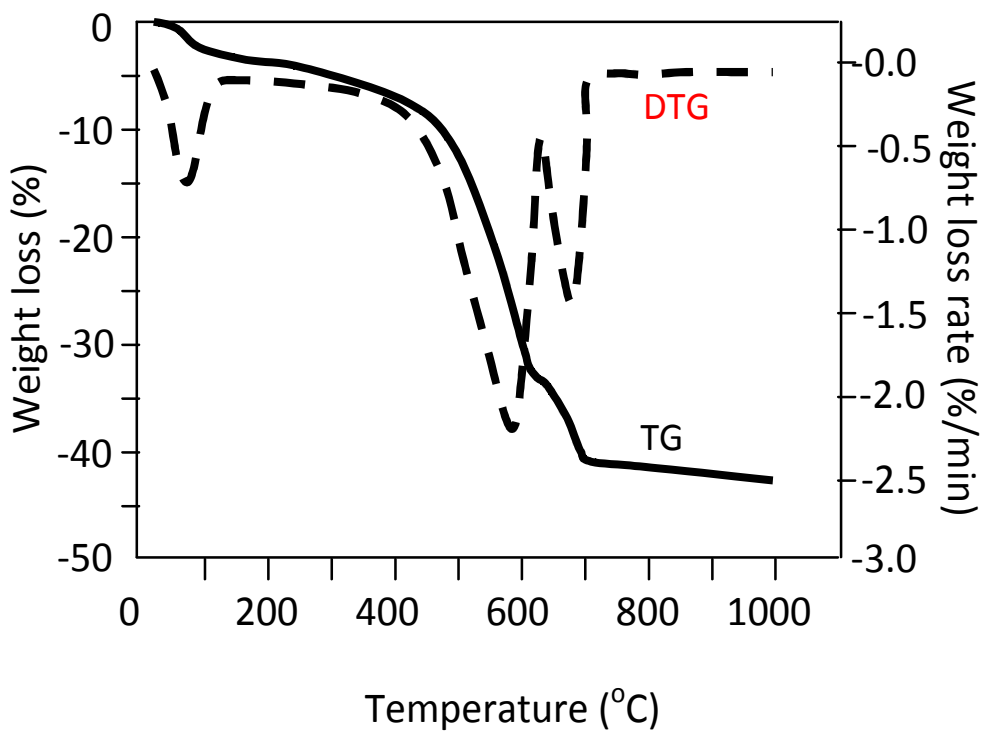


Figure 8a

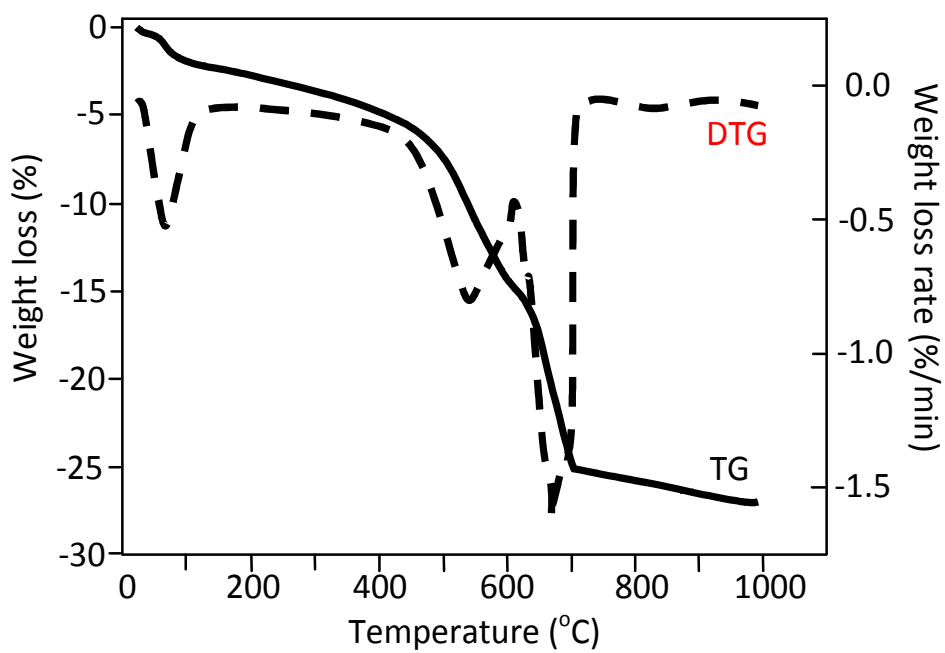


Figure 8b